

# In-Place Printing of Flexible Electrolyte-Gated Carbon Nanotube Transistors With Enhanced Stability

Jorge A. Cardenas<sup>1</sup>, Student Member, IEEE, Shiheng Lu, Nicholas X. Williams, James L. Doherty, and Aaron D. Franklin<sup>1</sup>, Senior Member, IEEE

**Abstract**—Ion gel-based dielectrics have long been considered for enabling low-voltage operation in printed thin-film transistors (TFTs), but their compatibility with in-place printing (a streamlined, direct-write printing approach where devices never leave the printer mid- or post-process) remains unexplored. Here, we demonstrate a simple and rapid 4-step in-place printing procedure for producing low-voltage electrolyte-gated carbon nanotube (CNT) thin-film transistors at low temperature (80 °C). This process consists of the use of polymer-wrapped CNT inks for printed channels, silver nanowire inks for printed electrodes, and imidazolium-based ion gel inks for printed gate dielectrics. We find that the efficacy of rinsing CNT films and printing an ion gel in-place is optimized using an elevated platen temperature (as opposed to external rinsing or post-process annealing), where resultant devices exhibited on/off-current ratios exceeding  $10^3$ , mobilities exceeding  $10 \text{ cm}^2\text{V}^{-1}\text{s}^{-1}$ , and gate hysteresis of only 0.1 V. Additionally, devices were tested under mechanical strain and long-term bias, showing exceptional flexibility and electrochemical stability over the course of 14-hour bias tests. The findings presented here widen the potential scope of print-in-place (PIP) devices and reveal new avenues of investigation for the improvement of bias stress stability in electrolyte-gated transistors.

**Index Terms**—Carbon nanotubes, thin-film transistors, silver nanowires, ion gel dielectric, aerosol jet printing, low-temperature printing, print-in-place.

## I. INTRODUCTION

FULLY direct-write printed electronics have the potential to accelerate the growth of the internet of things (IoT) through the rapid development of highly customized systems [1]–[3]. Though numerous embodiments of fully direct-write printed electronics have been demonstrated [4]–[8], the fabrication processes remain laborious and time-consuming due to the multilayer complexity of electronic systems and the manual post-process steps required to achieve

the desired electronic properties for each layer. Despite intensive research efforts, streamlined direct-write print processes, or “in-place” printing (where devices remain in-place within the printer throughout the entire fabrication process and do not require external mid- or post-processing), have been sparsely demonstrated. The challenges associated with print-in-place (PIP) devices can be largely attributed to the high process temperature requirements imposed by the electronic materials and inks involved.

Semiconducting carbon nanotubes (s-CNTs) are one of the preeminent semiconductor materials for enabling fully printed IoT systems [9]–[12]. Compared to other printable semiconductors, such as those composed of organics or metal-oxides, s-CNT films have both greater carrier mobilities and greater compatibility with low-temperature solution processing [13]–[16], making them an excellent candidate for PIP thin-film transistors (TFTs). Yet there remain many challenges facing the in-place printing of carbon nanotube thin-film transistors (CNT-TFTs), largely involving the low-temperature process compatibility of the surrounding electrodes and gate dielectric.

A critical first step toward PIP CNT-TFTs was the development of high-conductivity metallic electrodes compatible with rapid printing at low temperatures ( $< 80 \text{ }^\circ\text{C}$ ) facilitated by silver nanowires (AgNWs) as opposed to nanoparticles (AgNPs) [17], [18]. This led to the demonstration of a PIP process for establishing s-CNT and silver films with low contact resistance in CNT-TFTs [19], [20]. For gate dielectrics, Lu, *et al.* [21] developed a low-temperature compatible hexagonal boron nitride (h-BN) dielectric ink for fully in-place printed devices. However, due to the large thickness of printed films, transistors with printed gate dielectrics often require high operating voltages, limiting their potential for use in low-voltage applications.

Electrolytic dielectrics and imidazolium-based ion gels have long been considered for use in CNT-TFTs for low-power and low-frequency applications [22]–[27]. However, the compatibility of an ion gel with low-temperature, in-place printing remains questionable due to the presence of excess water and ink solvent molecules that can be trapped within the ion gel and at the semiconductor interface [28]. Still, even if ion gel inks are compatible with in-place printing, the electrochemical stability of the resultant devices remains questionable as

Manuscript received December 19, 2020; revised January 16, 2021 and January 23, 2021; accepted January 24, 2021. Date of publication February 1, 2021; date of current version February 24, 2021. This work was supported by the National Institutes of Health under Grant 1R01HL146849. The review of this letter was arranged by Editor S. Hall. (Corresponding author: Aaron D. Franklin.)

The authors are with the Department of Electrical and Computer Engineering, Duke University, Durham, NC 27708 USA (e-mail: aaron.franklin@duke.edu).

Color versions of one or more figures in this letter are available at <https://doi.org/10.1109/LED.2021.3055787>.

Digital Object Identifier 10.1109/LED.2021.3055787

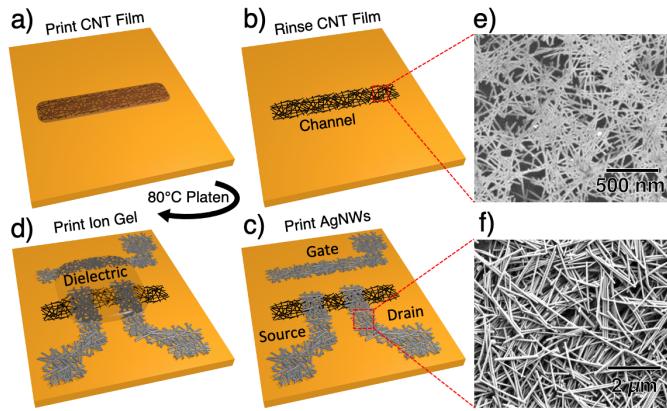


**Fig. 1.** Process flow for fully print-in-place (PIP) CNT-TFTs. **a)** Printed polymer-wrapped s-CNT film with excess organics. **b)** A more pristine s-CNT film resulting from an in-place rinsing process. **c)** Electrodes that are all printed in a single step, after which are immediately conductive. **d)** Printed ion gel gate dielectric yielding complete devices ready for test. Representative scanning electron micrographs of printed **e)** s-CNT films and **f)** AgNW films.

recent studies have shown that electrolyte-gated CNT-TFTs with AgNP electrodes significantly degrade after only 20–30 minutes of continuous bias [29].

In this work, we develop a simple and rapid 4-step, PIP process for producing low-voltage electrolyte-gated CNT-TFTs at low temperature (80 °C) using s-CNTs, AgNWs, and imidazolium-based ion gel inks. The efficacy of printing ion gels and rinsing s-CNT films in-place is investigated, with the process for each optimized using an elevated platen temperature. The resultant devices were exceptionally flexible and stable over the course of 14-hour continuous bias tests.

## II. DEVICE FABRICATION AND PRINTING

All devices were fabricated on 127- $\mu\text{m}$ -thick Kapton substrates cleaned in an isopropanol ultrasonic bath for 5 minutes, rinsed with water, and dried using  $\text{N}_2$ . Once the substrates were cleaned, they were placed on the printer platen (heated to 80 °C) and were only removed upon completion of the fabrication process, when they were ready for immediate testing. Fig. 1 outlines a simple and rapid, 4-step printing procedure for an Optomec AJ300 aerosol jet printer, where each step is carried out sequentially, in air on an 80 °C platen. Device dimensions were channel length and width of  $L_{\text{Ch}} = 100 \mu\text{m}$  and  $W_{\text{Ch}} = 300 \mu\text{m}$ , respectively.

The s-CNT channel was printed first, using a toluene-dispersed, polymer-wrapped s-CNT ink (IsoSol-S100, Nanointegris Inc.). A s-CNT concentration of 20  $\mu\text{g}/\text{mL}$  was used with 1% terpineol added to improve the uniformity of ink evaporation [30]. Films were printed using a nozzle diameter of 150  $\mu\text{m}$ , a print speed of 1 mm/s, a sheath gas flow rate (ShGF) of 40 sccm, a carrier gas flow rate (CGF) of 23 sccm, and an ultrasonic transducer current (UC) of 320 mA.

The resulting film contained excess polymer and terpineol (as illustrated in Fig. 1a). A toluene rinse was used to remove the remnant ink additives, which was carried out directly on the 80 °C printer platen in an in-place manner as opposed to the traditional procedure of removing the sample from the printer to rinse externally under a fume hood. The in-place rinsed samples were dried using an  $\text{N}_2$  gun where toluene

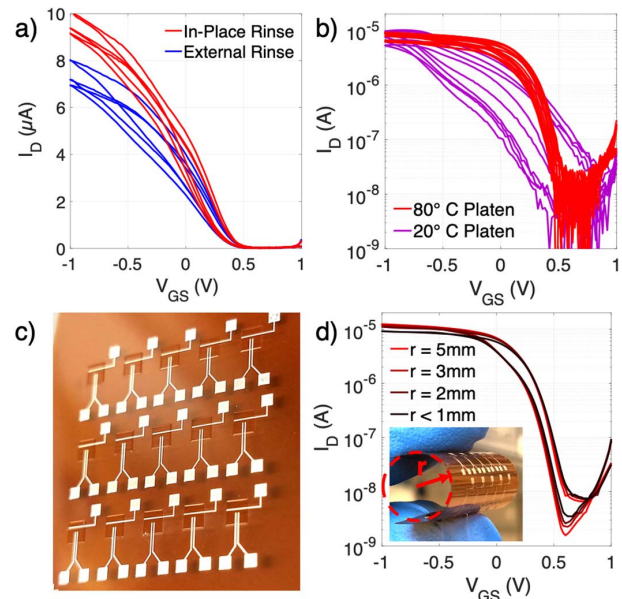


**Fig. 2.** Performance of PIP CNT-TFTs ( $V_{\text{DS}} = -0.1\text{V}$ ). **a)** Transfer curves of in-place versus externally rinsed s-CNT films. **b)** Subthreshold curves of devices with ion gels printed at 80 °C and 20 °C. **c)** Image of an array of in-place printed CNT-TFTs. **d)** Subthreshold curves of devices under various radii of applied bending. All devices have  $L_{\text{Ch}} = 100 \mu\text{m}$  and  $W_{\text{Ch}} = 300 \mu\text{m}$ .

from the rinse quickly evaporated due to the  $\text{N}_2$  flow and the elevated platen temperature, giving rise to a more pristine s-CNT film, shown in Fig. 1e. Not only can this in-place rinsing process be carried out in an automated manner, but it also results in more efficient polymer removal from the s-CNT film.

Next, silver contacts and gate electrodes were printed from a water-based AgNW ink in an offset gate configuration (as shown in Fig. 1c and 1f), enabling the contacts and gate to be printed in the same step. To prepare AgNW ink, 4- $\mu\text{m}$ -long nanowires were synthesized according to the polyol method [17] and dispersed into water at 10 mg/mL. Hydroxypropyl methylcellulose (HPMC) and propylene glycol (PG) were added to the AgNW dispersion in concentrations of 0.09 mg/mL and 3.8% w/w, respectively, in order to modify ink rheology and improve pattern morphology. Films were printed using a nozzle diameter of 200  $\mu\text{m}$ , a print speed of 2 mm/s, a ShGF of 25 sccm, a CGF of 35 sccm, and a UC of 370 mA.

Finally, an ion gel dielectric was printed over the channel, gate, and contacts (Fig. 1d) from an ink consisting of triblock polymer PS-PMMA-PS, ionic liquid EMIM-TFSI, and ethyl acetate in a 2:8:90 w/w ratio. Films were printed using a nozzle diameter of 150  $\mu\text{m}$ , a print speed of 3 mm/s, a ShGF of 25 sccm, a CGF of 20 sccm, and a UC of 320 mA. Contrary to typical electrolyte-gated CNT-TFTs, resultant devices required neither additional curing time nor post-process vacuum annealing, and were functional immediately after printing. All device measurements were carried out in air at room temperature.

## III. RESULTS AND DISCUSSION

The effects of an in-place toluene rinse versus an external room-temperature rinse are examined through the transfer

characteristics in Fig. 2a. In-place rinsed devices consistently exhibited slightly higher on-currents and transconductances compared to externally rinsed devices due to the thermal energy supplied by the printer platen during the toluene rinse, which aids in polymer removal. In previous work, larger radial breathing mode (RBM) Raman peaks were observed from in-place rinsed s-CNT films, likely resulting from a greater ability of s-CNTs to expand and contract during Raman excitation (suggesting those s-CNTs were less confined by wrapping-polymers) [19]. In addition to having higher on-currents, in-place rinsed devices also exhibited approximately a 74% decrease in hysteresis between forward and backward gate sweeps.

In addition to in-place rinsing, the 80 °C platen temperature was also key to processing the printed ion gel, as is shown in the subthreshold curves in Fig. 2b. Compared to devices with ion gels printed at room temperature (hysteresis = 0.5V and SS = 320 mV/dec), devices with ion gels printed on an 80 °C platen resulted in much smaller hysteresis (< 0.1 V) and much steeper subthreshold swing (SS = 90 mV/dec). Even when room temperature-printed ion gels were baked at 150°C after printing, their SS would improve briefly, but then return to their original state. This finding suggests that printing the ion gel on a heated surface aids in driving off residual water and solvent vapors that would otherwise become trapped within the gel, in its bulk or near the semiconductor interface. Furthermore, ion gels printed at 80 °C and 20 °C exhibited ionic conductivities of 4.8 mS/cm and 0.4 mS/cm, respectively, which may suggest that the heated platen aids in the self-assembly of the film upon deposition.

An image of an array of the resulting flexible CNT-TFTs can be seen in Fig. 2c, along with the operation of a representative device in Fig. 2d, measured while subject to varying degrees of applied strain. It can be seen that from 5 to 2 mm bending radii, the device exhibits minimal changes in response to the applied strain. It is not until the substrate was bent to a radius less than 1 mm that a more noticeable drop in performance occurs.

Even though s-CNTs themselves have been shown to be stable over long-term periods of bias stress [31], previous studies using ion gel dielectrics and AgNP electrodes have reported poor bias stability; *i.e.*, device failure occurred over the course of only 20-30 minutes ( $V_{GSbias} = -0.8V$ ) [29]. Here, our devices are continuously biased for up to 14 hours without significant electrochemical degradation.

When large fixed bias voltages ( $V_{GSbias} = -0.8V$ ) are applied, devices exhibit a small but distinct drop in on-current over the course of the test, dropping by only 10% over that period of time. However, under these high-bias conditions, the majority of the degradation observed occurred in the off-state, determined through measurements of the subthreshold characteristics before and after the test (Fig. 3b). When devices were subjected to intermediate fixed bias voltages ( $V_{GSbias} = -0.2V$ ) within the device's on-state, the drain current remains constant over the entire course of the test. Furthermore, 14-hour bias tests at these intermediate bias voltages have very little impact on the overall characteristics of the device (Fig. 3c). This is also the case when devices are

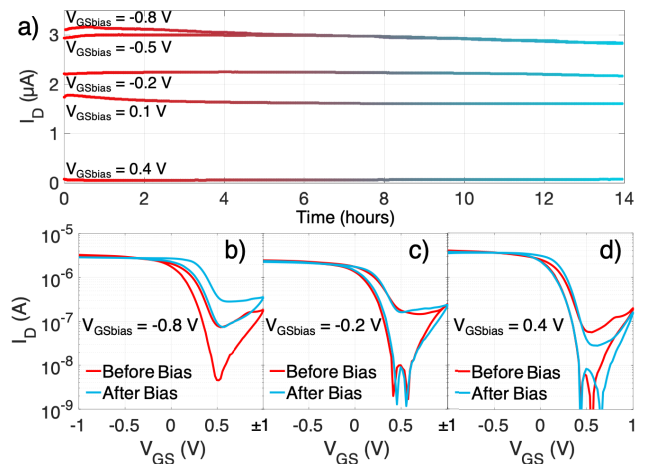


Fig. 3. Continuous bias stress stability of in-place printed CNT-TFTs ( $V_{DS} = -0.1V$ ). a) 14-hour continuous bias test. Subthreshold curves before and after 14-hour bias test at b)  $V_{GSbias} = -0.8V$ , c)  $V_{GSbias} = -0.2V$ , d)  $V_{GSbias} = 0.4V$ . All devices have  $L_{Ch} = 100 \mu m$  and  $W_{Ch} = 300 \mu m$ .

biased in their off-state (Fig. 3d), where very little change to the transistor characteristics is observed.

Though further investigation is warranted, improvements in bias stress stability that we report may be attributable to the elevated platen temperature used throughout printing, which dispelled water molecules from the bulk of the ion gel and at the AgNW interface, resulting in slower electrochemical reaction rates. Though AgNWs were primarily used in this work, similar results were also found using AgNP contacts, suggesting that the silver morphology does not play a large role in the enhancement in long-term stability seen in this work.

In future work, an emphasis on the improvement of device on/off ratios should be focused on in addition to print-to-print consistency. Though device characteristics in this work exhibited favorable consistency on small substrates, further work is needed to enhance print-to-print and batch-to-batch consistency over larger substrates for large-area applications. Along these lines, the development of an automated in-place rinsing process would greatly improve uniformity within and across prints. Additionally, further work is needed to understand the mechanism of improved stability and how the interface between CNT films, silver films, and ion gels impacts device performance. Overall, this work demonstrates the efficacy of in-place printed, electrolyte-gated CNT-TFTs while improving their stability and reveals new avenues of investigation for bias stress stability in electrolyte-gated transistors.

#### IV. CONCLUSION

In summary, an in-place printing process for producing low-voltage electrolyte-gated CNT-TFTs at low temperature was demonstrated using s-CNTs, AgNWs, and an imidazolium-based ion gel. High performing ion gel-based devices were printed in-place, and the resulting devices were tested under both mechanical strain and long-term bias, showing exceptional resilience to these non-ideal conditions, despite being printed at low temperature using a simple and rapid 4-step PIP process.

## REFERENCES

- [1] J. Veres, R. D. Bringans, E. M. Chow, J. P. Lu, P. Mei, S. E. Ready, D. E. Schwartz, and R. A. Street, "Additive manufacturing for electronics 'beyond moore,'" in *IEDM Tech. Dig.*, 2017, p. 25.
- [2] Y. Gu, D. Park, D. Bowen, S. Das, and D. R. Hines, "Direct-write printed, solid-core solenoid inductors with commercially relevant inductances," *Adv. Mater. Technol.*, vol. 4, no. 1, Jan. 2019, Art. no. 1800312.
- [3] A. A. Gupta, A. Bolduc, S. G. Cloutier, and R. Izquierdo, "Aerosol jet printing for printed electronics rapid prototyping," in *Proc. IEEE Int. Symp. Circuits Syst.*, May 2016, pp. 866–869.
- [4] L. Cai, S. Zhang, J. Miao, Z. Yu, and C. Wang, "Fully printed stretchable thin-film transistors and integrated logic circuits," *ACS Nano*, vol. 10, no. 12, pp. 11459–11468, Dec. 2016.
- [5] R. Worsley, L. Pimpolari, D. Mcmanus, N. Ge, R. Ionescu, J. A. Wittkopf, A. Alieva, G. Basso, M. Macucci, G. Iannaccone, K. S. Novoselov, H. Holder, G. Fiori, and C. Casiraghi, "All-2D material inkjet-printed capacitors: Toward fully printed integrated circuits," *ACS Nano*, vol. 13, no. 1, pp. 54–60, Jan. 2019.
- [6] H. Li, Y. Tang, W. Guo, H. Liu, L. Zhou, and N. Smolinski, "Polyfluorinated electrolyte for fully printed carbon nanotube electronics," *Adv. Funct. Mater.*, vol. 26, no. 38, pp. 6914–6920, Oct. 2016.
- [7] S. A. Singaraju, T. T. Baby, F. Neuper, R. Kruk, J. A. Hagmann, H. Hahn, and B. Breitung, "Development of fully printed electrolyte-gated oxide transistors using graphene passive structures," *ACS Appl. Electron. Mater.*, vol. 1, no. 8, pp. 1538–1544, Aug. 2019.
- [8] J. Chen, S. Mishra, D. Vaca, N. Kumar, W.-H. Yeo, S. Sitaraman, and S. Kumar, "Thin dielectric-layer-enabled low-voltage operation of fully printed flexible carbon nanotube thin-film transistors," *Nanotechnology*, vol. 31, no. 23, Mar. 2020, Art. no. 235301.
- [9] K. Chen, W. Gao, S. Emaminejad, D. Kiriya, H. Ota, H. Y. Y. Nyein, K. Takei, and A. Javey, "Printed carbon nanotube electronics and sensor systems," *Adv. Mater.*, vol. 28, no. 22, pp. 4397–4414, Jun. 2016.
- [10] W. A. G. Rojas and M. C. Hersam, "Chirality-enriched carbon nanotubes for next-generation computing," *Adv. Mater.*, vol. 32, no. 41, Oct. 2020, Art. no. 1905654.
- [11] J. Sun, A. Sapkota, H. Park, P. Wesley, Y. Jung, B. B. Maskey, Y. Kim, Y. Majima, J. Ding, J. Ouyang, C. Guo, J. Lefebvre, Z. Li, P. R. L. Malenfant, A. Javey, and G. Cho, "Fully R2R-printed carbon-nanotube-based limitless length of flexible active-matrix for electrophoretic display application," *Adv. Electron. Mater.*, vol. 6, no. 4, Apr. 2020, Art. no. 1901431.
- [12] X. Wang, M. Wei, X. Li, S. Shao, Y. Ren, W. Xu, M. Li, W. Liu, X. Liu, and J. Zhao, "Large-area flexible printed thin-film transistors with semiconducting single-walled carbon nanotubes for NO<sub>2</sub> sensors," *ACS Appl. Mater. Interfaces*, vol. 12, no. 46, pp. 51797–51807, 2020.
- [13] J. A. Cardenas, J. B. Andrews, S. G. Noyce, and A. D. Franklin, "Carbon nanotube electronics for IoT sensors," *Nano Futures*, vol. 4, no. 1, Jan. 2020, Art. no. 012001.
- [14] L. Nela, J. Tang, Q. Cao, G. Tulevski, and S.-J. Han, "Large-area high-performance flexible pressure sensor with carbon nanotube active matrix for electronic skin," *Nano Lett.*, vol. 18, no. 3, pp. 2054–2059, Mar. 2018.
- [15] G. L. Goh, S. Agarwala, and W. Y. Yeong, "Aerosol-jet-printed preferentially aligned carbon nanotube twin-lines for printed electronics," *ACS Appl. Mater. Interfaces*, vol. 11, no. 46, pp. 43719–43730, Nov. 2019.
- [16] Y. Yuan, X. Tang, L. Jiang, Y. Yang, Y. Zhou, and Y. Dong, "Convenient CNT-paper gas sensors prepared by a household inkjet printer," *ACS Omega*, vol. 5, no. 51, pp. 32877–32882, Dec. 2020.
- [17] I. E. Stewart, M. J. Kim, and B. J. Wiley, "Effect of morphology on the electrical resistivity of silver nanostructure films," *ACS Appl. Mater. Interfaces*, vol. 9, no. 2, pp. 1870–1879, 2017.
- [18] N. X. Williams, S. Noyce, J. A. Cardenas, M. Catenacci, B. J. Wiley, and A. D. Franklin, "Silver nanowire inks for direct-write electronic tattoo applications," *Nanoscale*, vol. 11, no. 30, pp. 14294–14302, 2019.
- [19] J. A. Cardenas, M. J. Catenacci, J. B. Andrews, N. X. Williams, B. J. Wiley, and A. D. Franklin, "In-place printing of carbon nanotube transistors at low temperature," *ACS Appl. Nano Mater.*, vol. 1, no. 4, pp. 1863–1869, Apr. 2018.
- [20] J. A. Cardenas, S. Upshaw, N. X. Williams, M. J. Catenacci, B. J. Wiley, and A. D. Franklin, "Impact of morphology on printed contact performance in carbon nanotube thin-film transistors," *Adv. Funct. Mater.*, vol. 29, no. 1, Jan. 2019, Art. no. 1805727.
- [21] S. Lu, J. A. Cardenas, R. Worsley, N. X. Williams, J. B. Andrews, C. Casiraghi, and A. D. Franklin, "Flexible, print-in-place 1D–2D thin-film transistors using aerosol jet printing," *ACS Nano*, vol. 13, no. 10, pp. 11263–11272, Oct. 2019.
- [22] B. Nketia-Yawson and Y.-Y. Noh, "Recent progress on high-capacitance polymer gate dielectrics for flexible low-voltage transistors," *Adv. Funct. Mater.*, vol. 28, no. 42, Oct. 2018, Art. no. 1802201.
- [23] P. Chen, Y. Fu, R. Aminirad, C. Wang, J. Zhang, K. Wang, K. Galatsis, and C. Zhou, "Fully printed separated carbon nanotube thin film transistor circuits and its application in organic light emitting diode control," *Nano Lett.*, vol. 11, no. 12, pp. 5301–5308, Dec. 2011.
- [24] M. Zhu, H. Xiao, G. Yan, P. Sun, J. Jiang, Z. Cui, J. Zhao, Z. Zhang, and L.-M. Peng, "Radiation-hardened and repairable integrated circuits based on carbon nanotube transistors with ion gel gates," *Nature Electron.*, vol. 3, no. 10, pp. 622–629, Oct. 2020.
- [25] F. Xu, M.-Y. Wu, N. S. Safron, S. S. Roy, R. M. Jacobberger, D. J. Bindl, J.-H. Seo, T.-H. Chang, Z. Ma, and M. S. Arnold, "Highly stretchable carbon nanotube transistors with ion gel gate dielectrics," *Nano Lett.*, vol. 14, no. 2, pp. 682–686, Feb. 2014.
- [26] M. Ha, J.-W.-T. Seo, P. L. Prabhurashi, W. Zhang, M. L. Geier, J. J. Renn, C. H. Kim, M. C. Hersam, and C. D. Frisbie, "Aerosol jet printed, low voltage, electrolyte gated carbon nanotube ring oscillators with sub-5  $\mu$ s stage delays," *Nano Lett.*, vol. 13, no. 3, pp. 954–960, Mar. 2013.
- [27] M. Ha, Y. Xia, A. A. Green, W. Zhang, M. J. Renn, C. H. Kim, M. C. Hersam, and C. D. Frisbie, "Printed, sub-3 V digital circuits on plastic from aqueous carbon nanotube inks," *ACS Nano*, vol. 4, no. 8, pp. 4388–4395, Aug. 2010.
- [28] H. Li and L. Zhou, "Effects of ambient air and temperature on ionic gel gated single-walled carbon nanotube thin-film transistor and circuits," *ACS Appl. Mater. Interfaces*, vol. 7, no. 41, pp. 22881–22887, Oct. 2015.
- [29] M. Robin, L. Portilla, M. Wei, T. Gao, J. Zhao, S. Shao, V. Pecunia, and Z. Cui, "Overcoming electrochemical instabilities of printed silver electrodes in all-printed ion gel gated carbon nanotube thin-film transistors," *ACS Appl. Mater. Interfaces*, vol. 11, no. 44, pp. 41531–41543, Nov. 2019.
- [30] M. Rother, M. Brohmann, S. Yang, S. B. Grimm, S. P. Schießl, A. Graf, and J. Zaumseil, "Aerosol-jet printing of polymer-sorted (6,5) carbon nanotubes for field-effect transistors with high reproducibility," *Adv. Electron. Mater.*, vol. 3, no. 8, Aug. 2017, Art. no. 1700080.
- [31] S. G. Noyce, J. L. Doherty, Z. Cheng, H. Han, S. Bowen, and A. D. Franklin, "Electronic stability of carbon nanotube transistors under long-term bias stress," *Nano Lett.*, vol. 19, no. 3, pp. 1460–1466, Mar. 2019.